

# Aerosol, Water Vapor, and Ozone Roles Linking Solar Radiation and Climate: Results from Recent Field Experiments

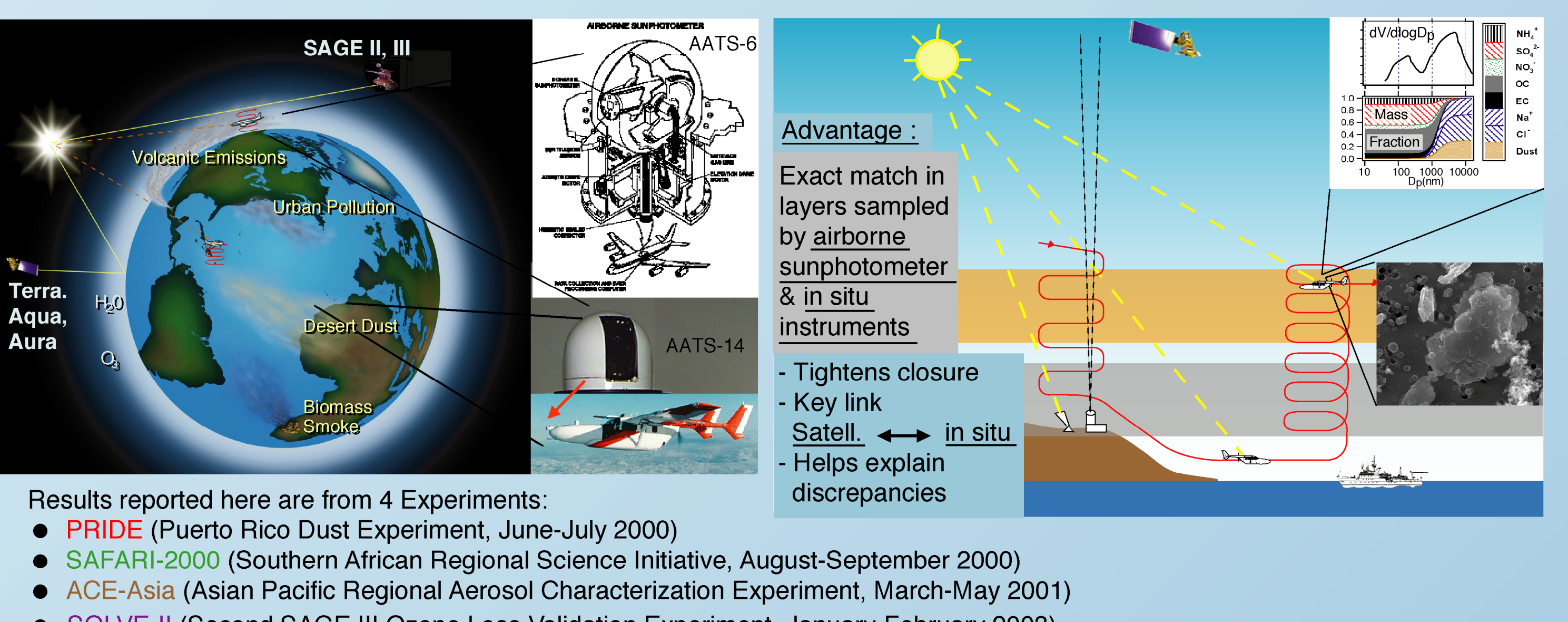
P. Russell<sup>1</sup>, J. Redemann<sup>2</sup>, B. Schmid<sup>2</sup>, J. Livingston<sup>3</sup>, P. Pilewskie<sup>1</sup>, R. Bergstrom<sup>2</sup>, S. Ramirez<sup>2</sup>, J. Eilers<sup>1</sup>, E. Welton<sup>4</sup>, C. Hsu<sup>5</sup>, R. Kahn<sup>6</sup>, R. Levy<sup>7</sup>, L. Remer<sup>4</sup>, A. Chu<sup>4</sup>, D. Hlavka<sup>7</sup>, P. Hobbs<sup>8</sup>, J. Campbell<sup>7</sup>, B. Holben<sup>4</sup>, M. McGill<sup>4</sup>, J. Reid<sup>9</sup>, T. Anderson<sup>8</sup>, S. Masonis<sup>8</sup>, A. Clarke<sup>10</sup>, S. Howell<sup>10</sup>, C. McNaughton<sup>10</sup>, B. Huebert<sup>10</sup>, J. Wang<sup>11</sup>, D. Collins<sup>12</sup>, J. Seinfeld<sup>11</sup>, R. Flagan<sup>11</sup>, H. Jonsson<sup>13</sup>, P. Colarco<sup>4</sup>, M. Chin<sup>4</sup>, O. Toon<sup>14</sup>, J. Anderson<sup>15</sup>, M. Bittner<sup>16</sup>, T. Erbertseder<sup>16</sup>

<sup>1</sup>NASA Ames Research Center, Moffett Field, CA <sup>2</sup>Bay Area Environmental Research Institute, Sonoma, CA <sup>3</sup>SRI International, Menlo Park, CA <sup>4</sup>NASA Goddard Space Flight Center, Greenbelt, MD <sup>5</sup>GEST/NASA Goddard Space Flight Center, Greenbelt, MD <sup>6</sup>Jet Propulsion Laboratory, Pasadena, CA <sup>7</sup>SSAI/NASA Goddard Space Flight Center, Greenbelt, MD <sup>8</sup>University of Washington, Seattle, WA <sup>9</sup>Naval Research Laboratory, Monterey, CA <sup>10</sup>University of Hawaii, Honolulu, HI <sup>11</sup>California Institute of Technology, Pasadena, CA <sup>12</sup>Texas A&M University, College Station, TX <sup>13</sup>Center for Interdisciplinary Remotely Piloted Aircraft Studies, Marina, CA <sup>14</sup>Laboratory for Atmospheric and Space Physics, University of Colorado, Boulder, CO <sup>15</sup>Arizona State University, Tempe, AZ <sup>16</sup>DLR (German Aerospace Center), Oberpfaffenhofen, Germany

## Scientific Motivation & Overall Approach

Aerosols caused by biomass burning, desert dust storms, urban pollution, and other processes form features recognizable from space on regional to intercontinental scales. These aerosols can change the climate by perturbing energy exchange between the sun, Earth, and space, as well as by redistributing energy within the atmosphere. Two gas-phase constituents, water vapor and ozone, are intimately involved in these processes, because they interact with aerosols both chemically and physically, and they are themselves major players in Earth's radiation budget. All three types of constituents—*aerosols*, water vapor, and ozone—can be retrieved quantitatively from spaceborne measurements. However, retrieval accuracy is still being determined, because it depends strongly on constituent type, measurement conditions, and spaceborne measurement technique.

The three constituent types can also be measured by airborne sunphotometry. Our work has emphasized the use of airborne sunphotometry as a unique link between space-based retrievals and a diversity of suborbital measurements. These include *in situ*, vertically resolved measurements of aerosol physico-chemical microproperties and radiative fluxes, as well as remote sensing by lidar and surface-based radiometers.

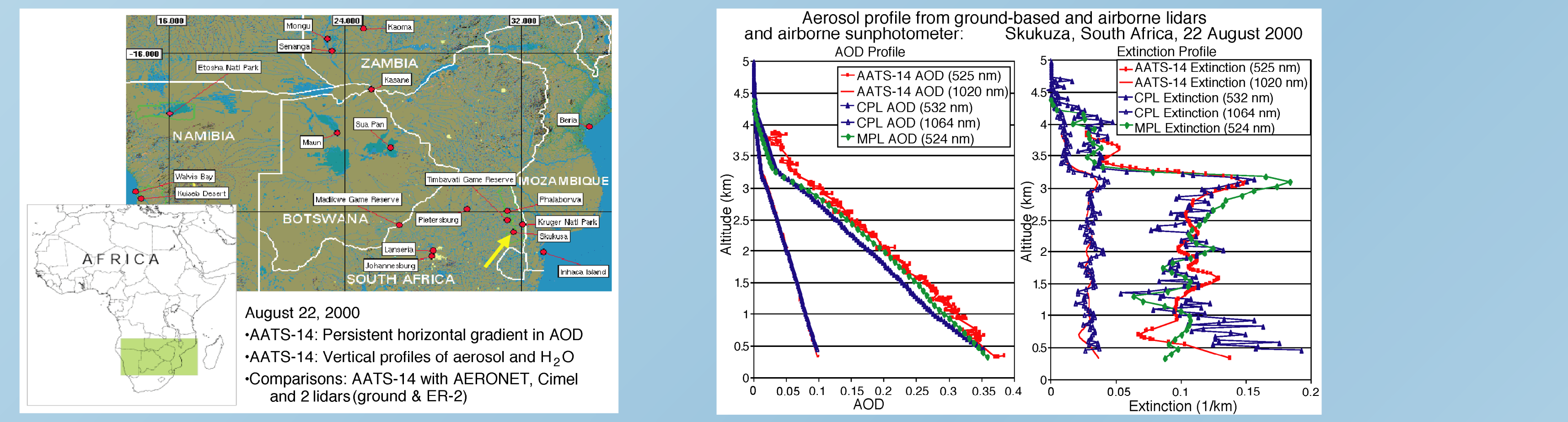


## 1. Satellite Validation

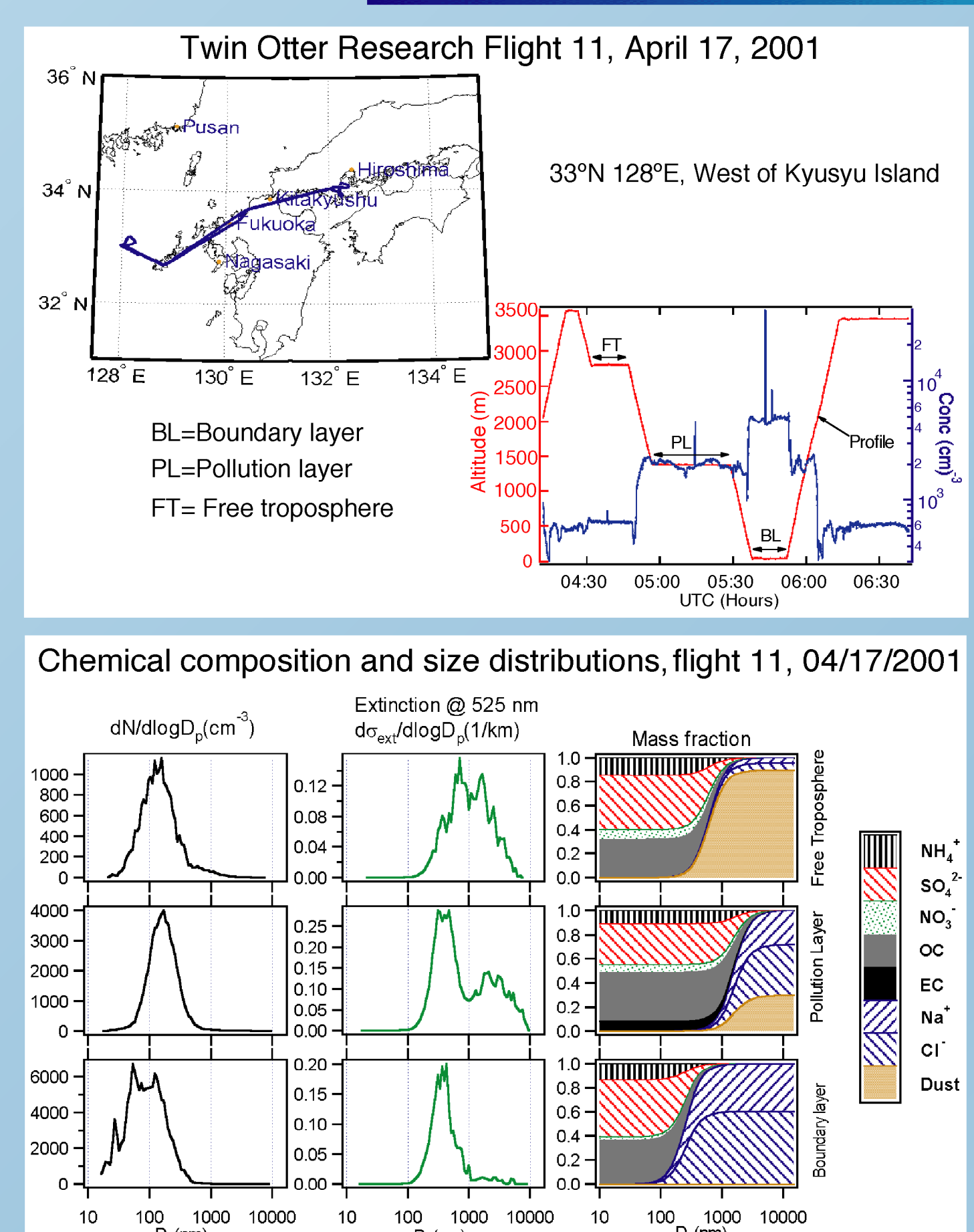
In PRIDE, SAFARI-2000, and ACE-Asia, the Ames Airborne Tracking Sunphotometers (AATS-6 and AATS-14) measured aerosol optical depth (AOD) spectra, coincident with satellite overpasses, for comparison to retrievals by AVHRR, GMS-5, GOES-8 Imager, MISR, MODIS, SeaWiFS, TOMS, and ATSR-2. Example comparisons are shown at right. These and related comparisons have shown:

- When dust is dominant ( $AOD > 0.2$  in Frame A), MODIS-retrieved AOD spectra slope more steeply than AATS AOD spectra. The likely cause is dust nonsphericity, which causes the MODIS retrieval to substitute more small mode aerosol for nonspherical large mode dust. An updated MODIS algorithm that adds nonspherical phase functions is being developed to address this.
- MODIS-AATS comparisons in SAFARI-2000 (Frame B) helped confirm that the biomass smoke SSA originally used in MODIS AOD retrievals ( $SSA \sim 0.9$ , based on SCAR-B) produced retrieved AODs < correlative AODs. Adopting a new SSA ( $\sim 0.85$ ) has now produced retrieved AODs (V4 MODIS in Frame B) that agree with AATS, AERONET, and other AODs in regions with strong biomass burning such as in Zambia.
- AATS-14 provided the first validation of MODIS-retrieved AODs at wavelengths 1.2 and 1.6 mm over water.
- MISR-AATS comparisons in SAFARI-2000 (Frame C) showed that a model including small, spherical, non-absorbing particles needed to be restored to the MISR retrieval. (It had been deleted early in the mission to reduce computer resource requirements.)
- MISR-AATS comparisons in ACE-Asia confirmed that early MISR-derived AODs were skewed high for some low-light-level scenes. Subsequent experiments demonstrated that scattered light played a key role in this phenomenon, and led to a revision of the MISR low-light-level calibration (that significantly affects MISR-derived AOD over dark water).
- An advanced SeaWiFS retrieval (4 wavelengths, 440 to 860 nm) produces AOD values over water that agree with airborne sunphotometer measurements to  $<0.04$ , a considerable improvement over the standard 2-wavelength SeaWiFS algorithm (Frame D).

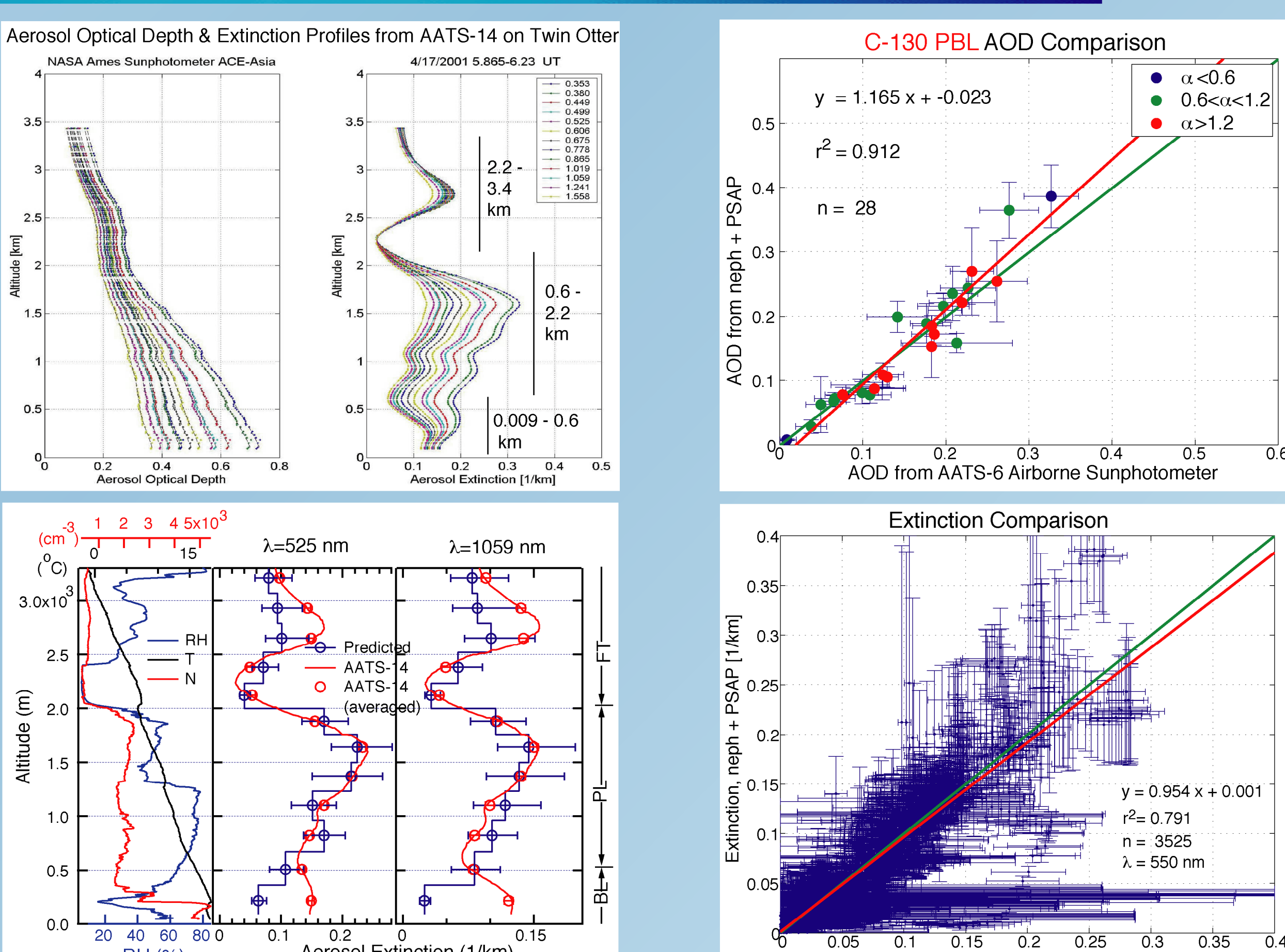
## 2. Closure Among Suborbital Results



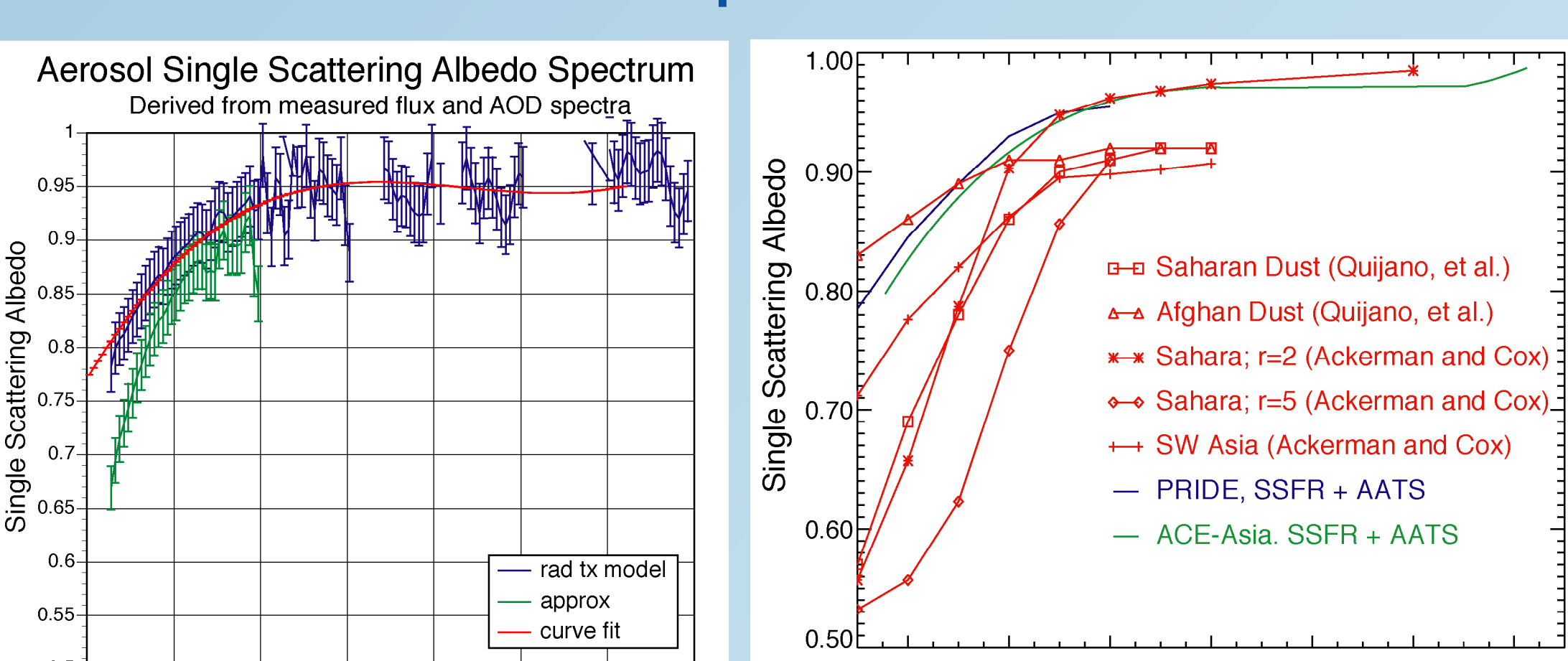
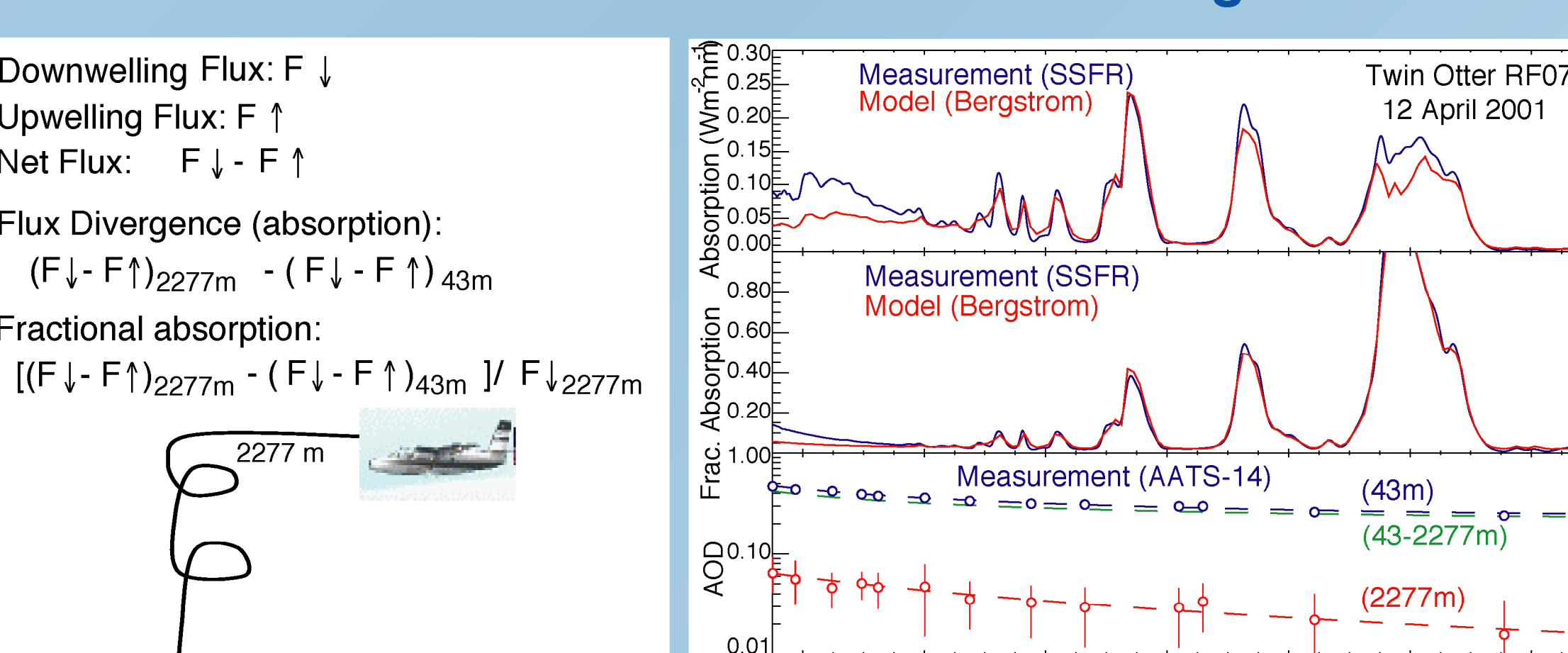
## SAFARI 2000



## ACE-Asia



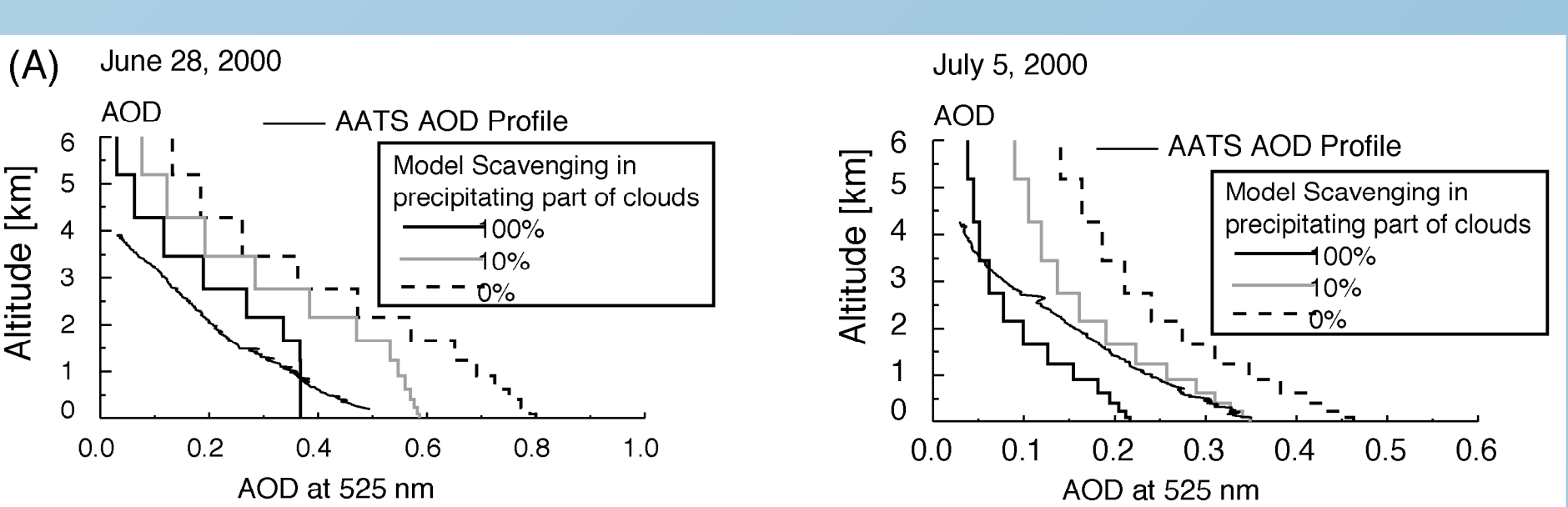
## 3. Aerosol Absorbing Fraction from Radiative Flux and AOD Spectra



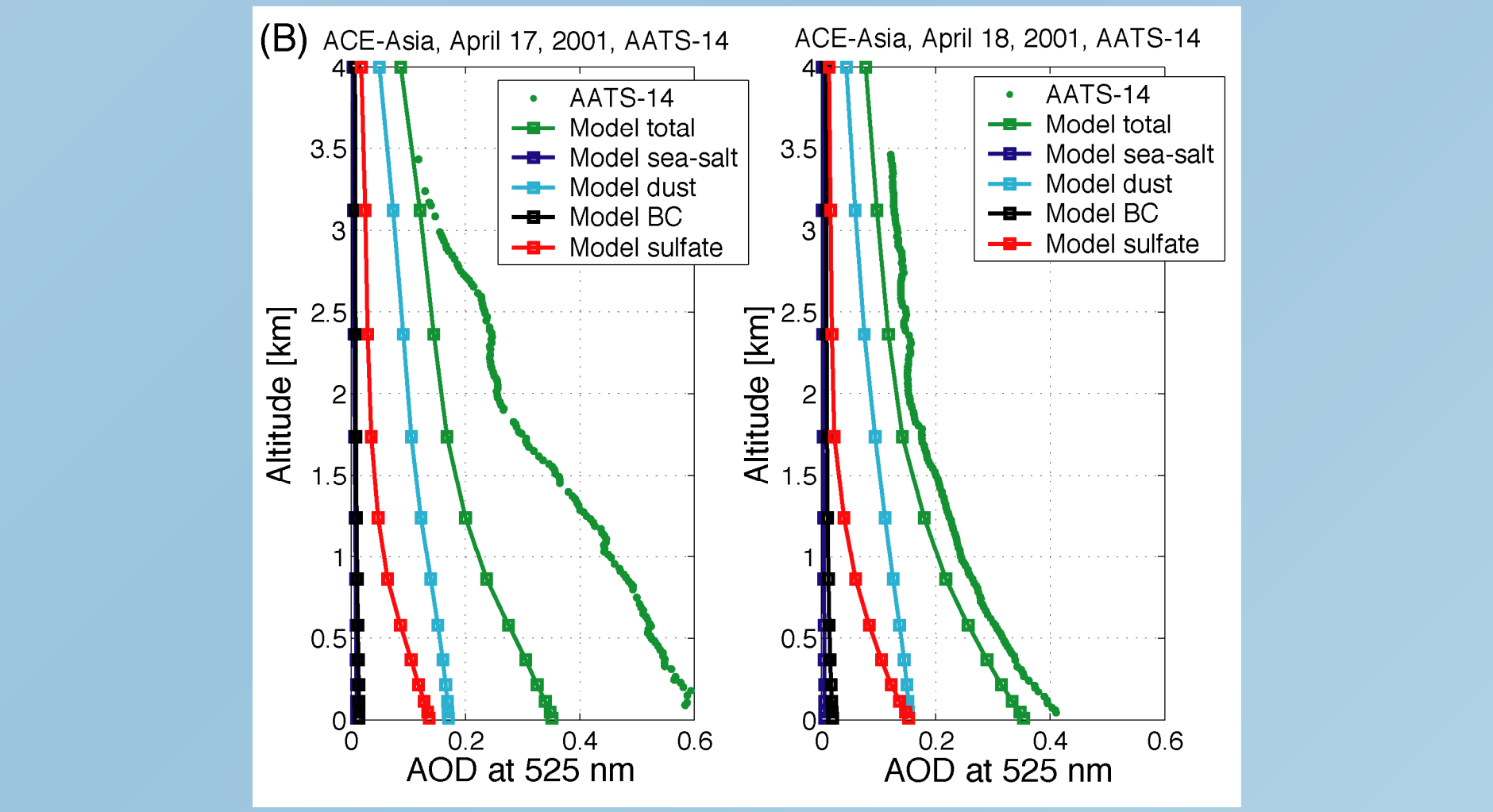
## 4. Tests of Chemical Transport Models

International comparisons of chemical-transport models (CTMs) show that aerosol vertical distributions often differ markedly from model to model. Hence, the vertical profiles of AOD and extinction measured by our airborne sunphotometers (AATS-6 and -14) can provide a key performance test for such CTMs. We have participated in such tests of the models GOCART, CARMA/MATCH, and MATCH.

Frame A shows examples of such comparisons between Sahara dust AOD profiles simulated by CARMA/MATCH and AOD profiles measured by AATS-6 in PRIDE. Both days, June 28 and July 5, 2000, are cases of low-level transport of Saharan dust to the Caribbean. The June 28 case shows poor agreement between measured and modeled AOD. The July 5 case shows good agreement below 1 km for model-assumed cloud scavenging of 10% in the precipitating part of clouds. Above that height, model calculations with more than 10% scavenging produce better agreement with AATS AOD.

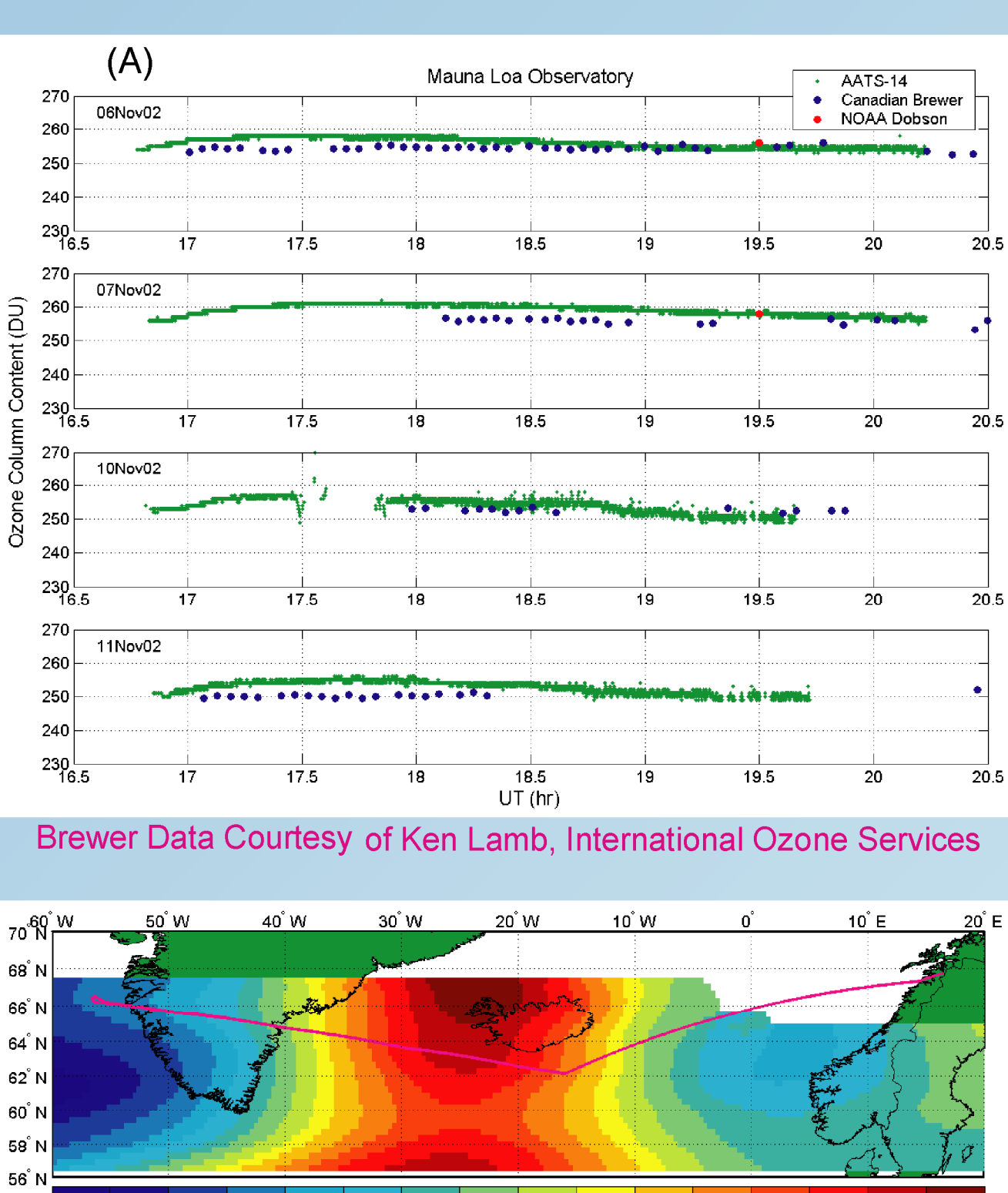


Frame B shows analogous comparisons between AOD profiles simulated by GOCART and measured by AATS-14 in ACE-Asia. Both days, April 17 and 18, 2001, are cases of mixed aerosols, treated in GOCART as height-dependent profiles of sulfate, soil dust, black carbon (BC), and sea salt. The April 18 case shows good agreement between measured and modeled total AOD profiles, especially in profile shape. In contrast, the April 17 case indicates that the model is underestimating one or more AOD components at the measurement time and location. Comparisons such as this are helping to guide model improvements.



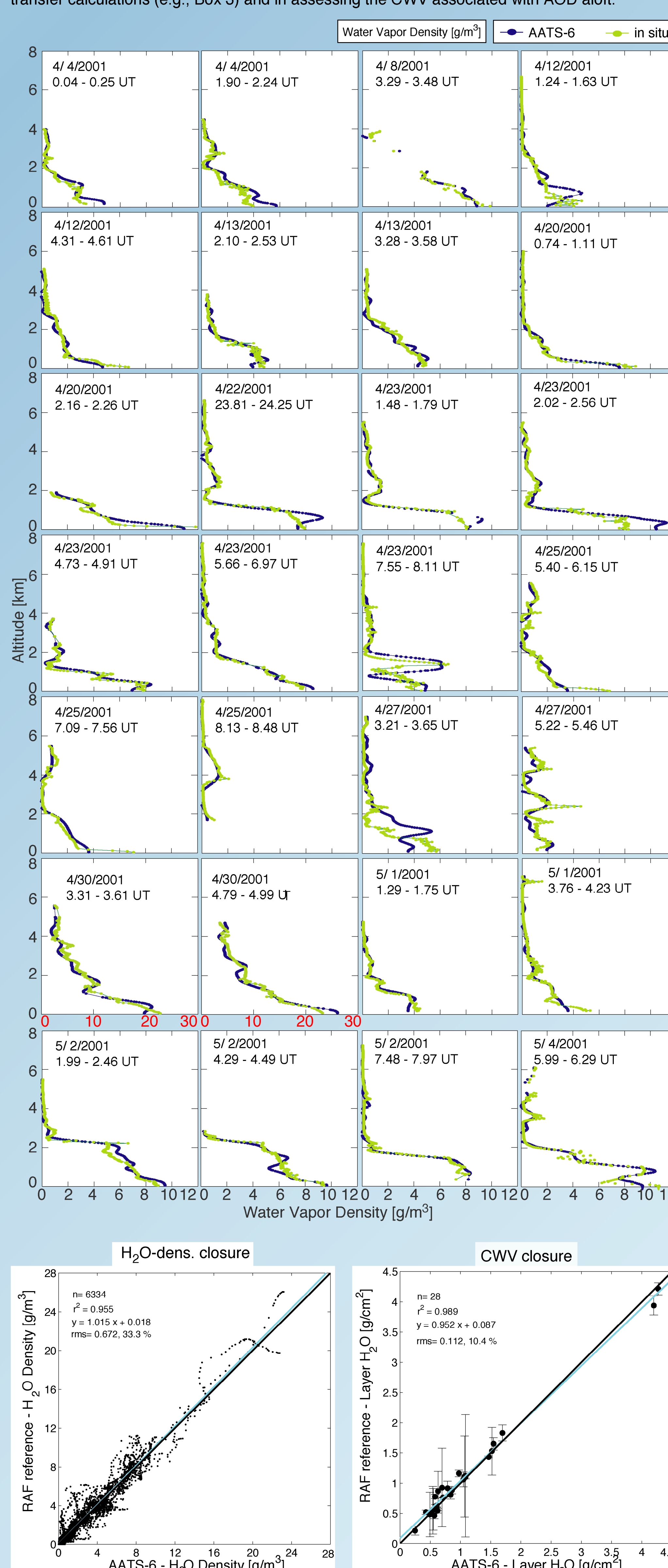
## 5. Ozone Spatial Structure and Comparisons

AATS-14 measures transmission at several channels in and around the Chappuis band, permitting retrieval of column ozone when AOD is sufficiently small. Comparisons (Frame A) between AATS-14, Brewer, and Dobson show differences of a few DU. Ozone spatial structure measured by AATS-14 on a DC-8 flight (Frame B) includes variations of  $\sim 100$  DU/ $20^\circ$  longitude near the polar vortex. The GOME results (from a harmonic analysis) agree well with AATS-14, though AATS-14 shows structure at finer scales than revealed by the GOME harmonic analysis.



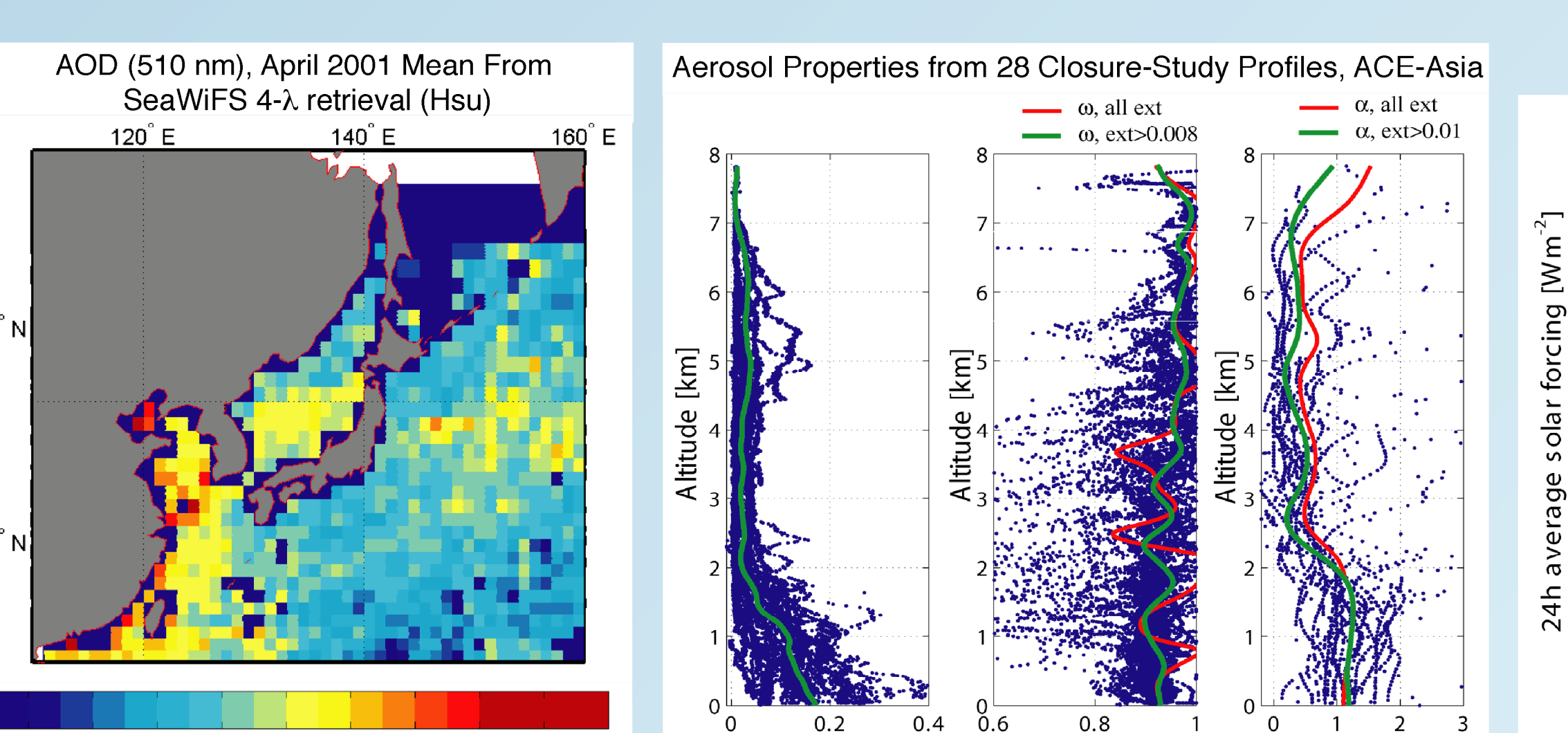
## 6. Water Vapor Comparisons

AATS-measured transmission in the 940-nm band and in surrounding channels is used to derive column water vapor (CWV). Vertical differentiation of CWV measured in profiles yields profiles of water vapor density. Comparisons to *in situ* measurements of both CWV and density yield the agreement shown. The continuously measured CWV results are useful in radiative transfer calculations (e.g., Box 3) and in assessing the CWV associated with AOD aloft.



## 7. Regional Forcing Assessments by Combining Satellite and Suborbital Results

We use several approaches in this subtask. The one shown here combines monthly-average SeawIFS-derived AOD with vertical profiles of aerosol intensive properties averaged from 28 closure-study profiles flown in ACE-Asia. These intensive properties yield the curves of forcing vs. AOD shown. Combining those curves with the SeaWiFS AOD map yields the forcing map shown.



## Summary and Conclusions

- Column AOD comparisons have helped improve retrievals by MODIS and MISR. Other comparisons have helped quantify the accuracy of AOD retrievals from AVHRR, GMS-5, GOES-8 Imager, SeaWiFS, TOMS, and ATSR-2.
- Extinction- and AOD-profile comparisons have quantified the ability of lidars and airborne *in situ* measurements to derive extinction from backscatter, from size distribution plus chemistry, and from scattering plus absorption. These comparisons provide independent tests of analysis methodologies, including inlet corrections for particle loss and enhancement (by evaporation, aerodynamics, etc.).
- Combining flux and AOD spectra yields SSA spectra from  $\sim 350$  to  $1600$  nm that are based on within-atmosphere solar absorption measurements and are free of any aerosol-sampling artifacts.
- Monthly average, cloud-free aerosol radiative forcing at the surface in ACE-Asia exceeded  $\sim 30$  W m $^{-2}$  in a plume downwind of Japan and in the Sea of Japan and Yellow Sea.